

molIEreVIS: Exploring and Interpreting the Evidence Behind Drug Repurposing Predictions

Amal Alnouri^{1*}, Andreas Hinterreiter¹, Christian Steinparz¹, Labinot Bajraktari², Sebastian Burgstaller-Muehlbacher³, Markus Bauer², Gregorio Alanis-Lobato³, and Marc Streit¹

¹ Visual Data Science Lab, Johannes Kepler University, Linz, Austria

² Boehringer Ingelheim RCV GmbH & Co KG, Vienna, Austria

³ Boehringer Ingelheim Pharma GmbH & Co KG, Biberach, Germany

Correspondence*:

Amal Alnouri

amal.alnouri@jku.at

2 Word count: 7,550 Figures: 9 Tables: 3

3 ABSTRACT

4 Finding new uses for existing drugs, known as drug repurposing, is a widely adopted drug
5 development strategy in the pharmaceutical industry. Computational drug repurposing leverages
6 vast biomedical data to prioritize repurposing candidates. Once these candidates are prioritized,
7 domain experts face the burden of evaluating their true potential. In this work, we propose a
8 visualization-based approach to address this challenge for a multimodal class of computational
9 drug repurposing, where heterogeneous evidence modalities are integrated. We conducted
10 a design study in close collaboration with domain experts, from which we derived a domain
11 abstraction of the expert assessment process. Grounded in this abstraction, we developed an
12 interactive visualization approach that explicitly models the expert reasoning process. We applied
13 the proposed approach to create a prototype implementation, molIEreVIS, in the context of
14 an operational drug repurposing pipeline. We used this prototype to collect qualitative feedback
15 from domain experts actively engaged in assessing computational drug repurposing candidates.
16 The results demonstrate the potential of our approach to support insights and reasoning in this
17 process and reveal directions for enhancements and future work.

18 **Keywords:** Drug Repurposing, Indication Expansion, Visualization, Knowledge Graph, Interpretability

1 INTRODUCTION

19 De novo drug development is known for its lengthy timelines, high attrition rates, and escalating costs (Hill
20 and Richards, 2021; Ashburn and Thor, 2004; Pushpakom et al., 2019; Pinzi et al., 2024). These challenges
21 have led drug developers to find new uses for existing drugs, a process known as drug repurposing (DR),
22 and offers the potential for a less risky development process, shorter timelines, and significantly lower
23 costs (Ashburn and Thor, 2004; Pushpakom et al., 2019; Pinzi et al., 2024). Drug repurposing used to be

24 opportunistic, which is the accidental discovery of an existing drug's activity in a new therapeutic context
25 (Pushpakom et al., 2019; Hamid et al., 2024).

26 In the era of big data, the vast availability of data from diverse sources has marked a turning point in
27 biomedical research (Cremin et al., 2022). Coupled with advances in computational approaches, nowadays,
28 computational drug repurposing formulates repurposing hypotheses by retrieving, integrating, and analyzing
29 such data sources to uncover the complex indirect relationships between drugs, biological targets, and
30 diseases (Pinzi et al., 2024; Saranraj and Kiran, 2025). It has transformed the traditional opportunistic
31 one-hypothesis-at-a-time process into a systematic and comprehensive exploration of possible repurposing
32 opportunities (Liu et al., 2013).

33 Still, these opportunities are less reliable than the ones prioritized by traditional approaches Cavalla
34 (2019), requiring careful assessment by domain experts to determine their true potential. This assessment
35 involves a detailed investigation of the biomedical evidence considered in the prioritization process. In this
36 work, we address this challenge through a visualization-based approach grounded in a design study we
37 carried out in close collaboration with domain experts.

38 To narrow down the scope of our contribution, it is necessary to consider the wide variety of computational
39 drug repurposing approaches, that differ substantially based on their underlying data sources (Tanoli et al.,
40 2025; Cousins et al., 2024; Kulkarni et al., 2023; Jarada et al., 2020; Pushpakom et al., 2019). Table 1
41 summarizes major repurposing approaches and their associated data modalities. Previous reviews (Pinzi
42 et al., 2024; March-Vila et al., 2017) have also emphasized the need to integrate different data modalities
43 toward a more comprehensive modeling of the complex interaction between biomedical entities, and to
44 overcome the inherent weaknesses of each when used alone. This work addresses the assessment challenge
45 for the multimodal class of computational drug repurposing, investigating how diverse lines of evidence
46 can be jointly explored and evaluated.

47 Previous research has recognized the importance of assessing computational drug repurposing candidates.
48 In general, studies that deliver computational repurposing candidates include a subsequent validation step
49 in which false positives are excluded and the overall performance of the repurposing method is evaluated.
50 Table 2 summarizes the validation strategies reviewed by Brown and Patel (2018) and Pillai and Wu (2024).
51 Several studies have been dedicated to developing automated validation approaches (Ozery-Flato et al.,
52 2020; Santamaría et al., 2021; Schatz et al., 2021; Nunes and Pesquita, 2024). Similar to the aforementioned
53 strategies, these approaches use existing biomedical data to contextualize the repurposing candidates with
54 additional evidence from existing knowledge. For instance, Nunes and Pesquita (2024) validate a single
55 drug repurposing candidate by finding k -shortest informative paths between the drug and the disease in
56 an independent knowledge graph. A key feature of this validation literature is that it focuses solely on
57 the outcomes of the validated methods rather than providing insights into the process behind them, and
58 relies on external data sources, rather than leveraging the evidence identified by the methods themselves.
59 Furthermore, it often summarizes findings into quantitative metrics, which, while useful, lack explanatory
60 depth and still requires expert interpretation.

61 In contrast, other works focus on developing self-explainable computational drug repurposing methods.
62 For instance, Gurbuz et al. (2022) and (Jiménez et al., 2024) developed inherently transparent repurposing
63 methods based on knowledge graphs. In their methods, candidates are directly underpinned by explicit
64 paths in the knowledge graph, which makes them interpretable by domain experts. Closely related research
65 to this work approaches this problem from a visualization and human-computer interaction perspective,
66 where a visualization design is proposed to support domain experts in assessing the prioritized candidates.

Table 1. Overview of computational drug repurposing approaches.

Based on	Data source	Description	Representative References
Structures	3D structures of biological targets	Molecular docking and binding affinity estimation	Ngernsombat et al. (2024); Khan et al. (2025); Lv et al. (2024); Iqbal et al. (2025)
Signatures	Molecular signatures derived from omics data (e.g., transcriptomics, proteomics)	Expression signature matching	Sun et al. (2025); Nikolakis et al. (2025)
Genetic associations	Genetic association data (e.g., Genome-wide association studies (GWASs))	Identification of disease-associated genetic variants	Seagle et al. (2025); Yu et al. (2024)
Networks	Interaction networks and multimodal knowledge graphs	Network propagation and link prediction	Chandak et al. (2023); Zhang et al. (2022)
Literature	Scientific literature	Literature mining for relationship discovery	Henry and McInnes (2017); Preiss (2025); Sikirzhyskaya et al. (2025)
Health data	Real-world health data	Real-world evidence mining	Adamek et al. (2024); Zang et al. (2023)

Table 2. Overview of computational drug repurposing validation strategies.

Strategy	Automated	Description
Retrospective clinical analysis	Yes	Searching real-world health data to identify off-label usage or clinical trial evidence
Literature mining	Yes	Analyzing biomedical literature to verify drug–indication connections
Benchmark datasets analysis	Yes	Validating candidates against benchmark datasets
Public database search	No	Manually searching public database (e.g., DrugBank (Wishart et al., 2008)) for drug–indication connections
Literature search	No	Manually searching through relevant scientific literature

67 In this context, we report two works that address the problem for the network-based repurposing approach,
68 where the candidates are prioritized by a graph neural network (GNN). Wang et al. (Wang et al., 2022;
69 Huang et al., 2024; Wang et al., 2021) developed DrugExplorer, which provides path-based explanations
70 using GraphMask, presenting them as both individual paths and aggregated paths (meta-paths). They also
71 proposed a novel visualization design, MetaMatrix, with interactive features that help domain experts

72 organize and compare explanation paths at different levels of granularity to generate domain-meaningful
73 insights. Similarly, HypoChainer (Jiang et al., 2025) traces paths in the knowledge graph to explain GNN
74 predictions. HypoChainer incorporates LLMs as a natural language interface for graph exploration. Experts
75 can ask a retrieval-augmented LLM about the rationale behind a prediction, and the response is based on
76 existing KG connections. In an iterative process, experts and the LLM collaboratively construct structured
77 reasoning paths. Finally, the workflow filters predictions based on alignment with KG-supported evidence.

78 While previous works proposed visualization designs to support domain experts in network-based drug
79 repurposing, our design study addresses this challenge for multimodal drug repurposing. We summarize
80 our contributions as follows:

- 81 • A domain abstraction of expert assessment in multimodal computational drug repurposing.
- 82 • A visualization-based approach that explicitly models how domain experts explore, interpret, and
83 validate drug repurposing candidates.
- 84 • A novel evidence provenance visualization that enables experts to trace evidence states through
85 successive transformations.
- 86 • A qualitative user study, demonstrating the potential of the proposed approach to support expert insight
87 generation and reasoning.

2 MATERIALS AND METHODS

88 This section provides a detailed overview of the methodologies we followed and materials we utilized to
89 derive and evaluate the proposed approach.

90 2.1 Design Study Outline

91 A team with complementary backgrounds in visualization and bioinformatics carried out the design study,
92 including computational drug repurposing experts who acted as domain intermediaries. The study followed
93 a two-stage process:

- 94 1. The first stage began with a workshop that laid the groundwork for a rough domain characterization,
95 introducing the workflow of multimodal drug repurposing pipelines, target users, challenges, and
96 practices in assessing computational drug repurposing candidates. From this point onward, the stage
97 adopted an iterative approach. Insights gained from the workshop informed initial domain and task
98 abstractions, as well as early conceptual design sketches, all of which were refined based on expert
99 feedback during regular meetings.
- 100 2. In the second stage, we instantiated the resulting design in a prototype implementation grounded in an
101 operational drug repurposing pipeline. The prototype was then tested by representative target users to
102 validate and reflect on the proposed design.

103 2.2 Domain Abstraction

104 This section presents our abstraction of the study domain, including the target users, their practices, and
105 data.

106 Through the close collaboration with domain experts, and informed by prior literature (McDonagh et al.,
107 2024; Steyaert et al., 2023; Ivanisevic and Sewduth, 2023; López de Maturana et al., 2019; Thorman

Table 3. Evidence transformation boundaries and data artifacts.

Boundary	Methods	Data Artifacts
Evidence collection	—	Qualitative evidence
Evidence quantification	Rule-based, model-based	Quantitative evidence
Evidence harmonization	E.g., saturation, normalization, projection in shared latent space	Harmonized evidence
Evidence integration	Rule-based, model-based	Consensus score, per-stream contribution

et al., 2024; Li and Ke, 2025), we model a multimodal drug repurposing pipeline, independent of how it is implemented, using the following four conceptual evidence transformation boundaries:

- Evidence collection:** *Qualitative evidence* is collected from diverse heterogeneous data sources.
- Evidence quantification:** Qualitative evidence is transformed into *quantitative evidence*, through manual feature extraction, learned modeling, or a combination of both.
- Evidence harmonization:** Quantitative evidence is aligned into a common representational space producing *harmonized evidence*, such that disparate modalities become comparable. This can be achieved, for instance, through saturation, normalization, or a shared latent space.
- Evidence integration:** multiple evidence modalities are integrated into a *consensus score* through methods spanning simple rule-based ones to advanced model-based ones. Regardless of the underlying method, evidence integration—either implicitly or explicitly—yields the *contribution* of each evidence modality to the consensus score.

These boundaries give rise to *data artifacts* that form a basis for a supportive visualization design. Table 3 summarizes these transformation boundaries and their corresponding data artifacts. The obtained consensus score is used to rank the repurposing hypotheses.

Some pipelines realize all boundaries explicitly, particularly those that quantify each evidence modality independently, then perform a distinct harmonization step before final integration. Other pipelines collapse the harmonization boundary directly into a model-based integration process, or they collapse both quantification and harmonization boundaries by applying early integration directly to qualitative evidence. When a pipeline collapses a boundary, the corresponding data artifacts also collapse.

Notably, our observations across prior literature suggest that this model is not specific to drug repurposing, but rather constitutes a general model for multimodal hypothesis generation across diverse computational drug discovery domains, including target prioritization and biomarker discovery.

The target users in our study are drug repurposing experts, ranging from wet-lab biologists with no familiarity with the computational pipeline processes to computational biologists with a conceptual understanding of its processes. The computer-aided repurposing process begins by selecting a single repurposing context (e.g., a drug) and querying the pipeline for candidates within that context. The post-prioritization assessment aims to shortlist candidates that deserve progression to subsequent laboratory validation. During this process, the former user group is able to examine prioritized hypotheses to identify promising candidates, while the latter user group is able to perform more in-depth computational analyses

138 and communicate their results to the former group to support collaborative decision-making. The domain
139 experts' reasoning model for the assessment process can be summarized in the following three-stage
140 analysis process, where an expert engages at a stage based on their expertise:

- 141 1. **Exploration:** Experts screen the ranked list of hypotheses in conjunction with the consensus score, and
142 would further benefit from examining per-stream contributions. At this stage, they look for potential
143 inconsistencies, such as misalignment with domain expectations, negligible differences in consensus
144 score magnitudes, or conflicting signals across evidence streams. Beyond the ranking, experts engage
145 in higher-level reasoning by interpreting consensus scores within domain ontologies (e.g., disease
146 ontologies). Furthermore, discussions with experts revealed that, when applicable, those who are
147 familiar with the pipeline processes would benefit from examining alternative scenarios at this stage,
148 for example, by disabling specific data streams or adjusting their relative influence. Such reasoning
149 allows experts to mitigate biases introduced by uneven evidence, including cases where literature-based
150 evidence is sparse, as in the study of “first-in-class” drugs with limited prior research. In addition, it
151 supports robustness validation. The outcome of this stage is a shortlist of candidate hypotheses for
152 further investigation.
- 153 2. **Interpretation:** Experts examine the qualitative evidence of the shortlisted candidates to assess
154 whether it provides a coherent and sound rationale for the candidate. Discussions with experts revealed
155 that those familiar with the pipeline processes would benefit from the ability to follow evidence through
156 the explicit transformation boundaries realized by the pipeline, as this enables more informed and
157 transparent judgments.
- 158 3. **Validation:** In line with established validation practices in the literature, experts validate the shortlisted
159 candidates by consulting external knowledge, typically a biomedical network. This stage contextualizes
160 the evidence in a broader domain understanding.

161 2.3 Design Goals

162 Guided by the outlined domain abstraction, we conclude the following design goals to embody the
163 experts' reasoning model and needs.

- 164 **DG1** *Support coarse-to-fine analysis*—The design should mirror the coarse-to-fine staged process followed
165 by domain experts to match their mental model and create an intuitive experience. Furthermore,
166 such a design in addition to adopting detail-on-demand principle in the individual stages, aligns the
167 interface with the user's immediate tasks, reducing cognitive load and increasing accessibility to
168 experts who are less familiar with the pipeline processes and may prefer to engage only at a coarse
169 level of analysis.
- 170 **DG2** *Directed analysis from query to candidate*—The analysis should start from the analysts' query and
171 allow them to constrain views to their shortlisted candidates.
- 172 **DG3** *Support evidence investigation*—Users should be able to examine the individual pieces of qualitative
173 evidence. In addition, the design should allow tracing evidence provenance from per-stream
174 contributions in the consensus score back to the underlying qualitative evidence, through the explicit
175 transformation boundaries realized by the pipeline.
- 176 **DG4** *Support consistency validation*—Validating the consistency of the biological relevance between the
177 query and the candidate in the context of broader curated knowledge should be an integral part of
178 the design.

179 **DG5** Support “what-if” analysis—The design should allow experts to explore how rankings change under
180 alternative “what-if” scenarios.

181 **DG6** Support ontology-informed analysis—The design should support the interpretation of results within
182 domain ontologies.

183 2.4 Operational Context: molIEre

184 Drug repurposing can be approached from three angles (Parisi et al., 2020; Thakur et al., 2024): (i
185) a **disease-centric** approach finds untreated diseases that share underlying biological pathways with an
186 established drug indication (the medical condition the drug is indicated for); (ii) a **drug-centric** approach
187 broadens the usage of an established drug by connecting it to a new biological target and its associated
188 indication; and (iii) a **target-centric**, approach—also known as **indication expansion (IE)** (Tanoli et al.,
189 2025)—pairs an established drug and its known biological target with a newly identified indication, where
190 the drug’s mode of action (MoA) also has a beneficial effect.

191 We evaluate our approach in the context of an operational indication expansion pipeline, called **molIEre**,
192 which is an unpublished pipeline in active use at *Boehringer Ingelheim*¹. The pipeline is initiated using
193 molecular targets of a known mode of action (MoA) and disease terms mapped across multiple ontologies.
194 It integrates multiple data streams, each of which consumes a different data source to collect supporting
195 or opposing evidence for the presumed association between the input MoA and the input disease. The
196 demonstrated version of the pipeline in this paper consumes data from three omics sources (genomics,
197 transcriptomics, proteomics) and one non-omics source (scientific literature).

198 **molIEre** quantifies each data source independently, then bounds the quantitative evidence into a shared
199 scale. Afterwards it integrates evidence modalities into a consensus score (M_{score}) using an expert-designed
200 weighted sum model. Figure 1 illustrates the complete workflow of **molIEre** which explicitly realizes all
201 the transformation boundaries in Table 3.

202 2.5 Technical Approach

203 The design instantiation, **molIEreVIS**, is a full-stack application composed of a frontend and a
204 backend. **molIEreVIS** requires as input the data artifacts produced by **molIEre**, for which we designed
205 a PostgreSQL database. The backend is a FastAPI server, that can query the PostgreSQL database.
206 Additionally, to support the validation stage logic (see Section 3.1.3), the backend dynamically queries
207 PrimeKG (Chandak et al., 2023), a knowledge graph stored in a Neo4j database, to retrieve paths between
208 entities and group them under meta-paths. The frontend of **molIEreVIS** was developed with React,
209 and we used D3.js to create custom visualizations. The source code is available at <https://github.com/jku-vds-lab/molierevis>, and our live demo can be tried out at <http://molierevis.jku-vds-lab.at/>.

212 One implementation challenge we encountered originated from the fact that **molIEre** candidate
213 indication names are drawn from the MeSH (U.S. National Library of Medicine, 2025) ontology, whereas
214 users need to query PrimeKG using these candidate names for validation. This required mapping disease
215 names between MeSH and the MONDO disease ontology (Shefchek et al., 2019) used by PrimeKG. To
216 address this, we implemented a fuzzy matching approach based on string similarity between disease
217 names. For a selected MeSH disease, we compute similarity scores against MONDO disease names in
218 PrimeKG and retain candidates above a predefined threshold. For example, the MeSH disease “*Pneumonia*,

¹ <https://www.boehringer-ingelheim.com>

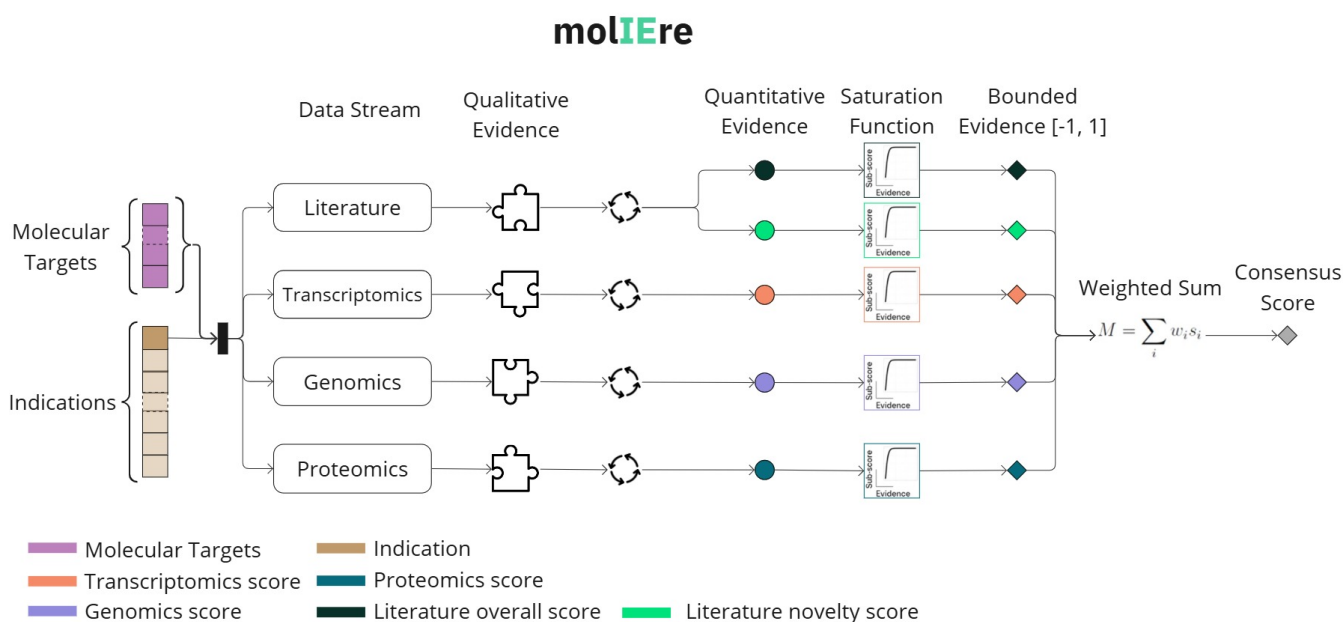


Figure 1. The operational indication expansion pipeline that contextualizes our study instantiation. The pipeline binds a consensus score (M_{score}) to a potential connection between a known MoA and a new indication. Using the molecular targets of an MoA and a disease term, it collects qualitative evidence from four independent data sources, which is subsequently quantified. Literature evidence yields two quantitative values: *novelty*, derived from recent publications, and *overall*, derived from all publications. The quantitative evidence is then saturated to produce a scalar harmonized evidence in the range $[-1, 1]$. Finally, the pipeline aggregates the bounded evidence through a weighted sum, yielding the final M_{score} .

219 *Bacterial*” is matched to the MONDO disease “*bacterial pneumonia*”, despite differences in word order and
 220 punctuation. These candidate matches are presented to the user, who can refine the selection by deselecting
 221 unrelated suggestions or selecting the most appropriate ones as needed.

222 2.6 User Study Setup

223 We conducted a qualitative user study with three domain experts occupying different functional roles at
 224 *Boehringer Ingelheim*. Their experience in the field ranges from two to four years, and all have experience
 225 in reading and creating charts. The participants’ familiarity with **molIERe** processes spans from good
 226 conceptual understanding to none, with **P1**, **P2**, and **P3** ordered accordingly. None of the study participants
 227 were involved in the design of our solution.

228 Before conducting the main user study, we ran a pilot study with one participant who was not involved
 229 later in the main study. The participant is a senior bioinformatician with three years of experience in the
 230 field, and has no connection to *Boehringer Ingelheim*. The pilot study helped us evaluate the preliminary
 231 version of our study protocol, and led us to refine both the study setup, as well as **molIEReVIS** design,
 232 particularly the design for adjusting the weights during the exploration stage (see Section 3.1.1).

233 We designed the study to evaluate the usefulness of **molIEReVIS** defined by Nielsen Norman Group
 234 (Nielsen, 2012) as a combination of: *usability* (how easily and effectively users can interact with the system)
 235 and *utility* (whether the system fulfills a specific need or solves a problem).

236 The study was conducted in isolated 70-minute sessions, one for each participant. To assess usability,
 237 we took structured notes throughout the sessions that documented usability difficulties, such as hesitation,

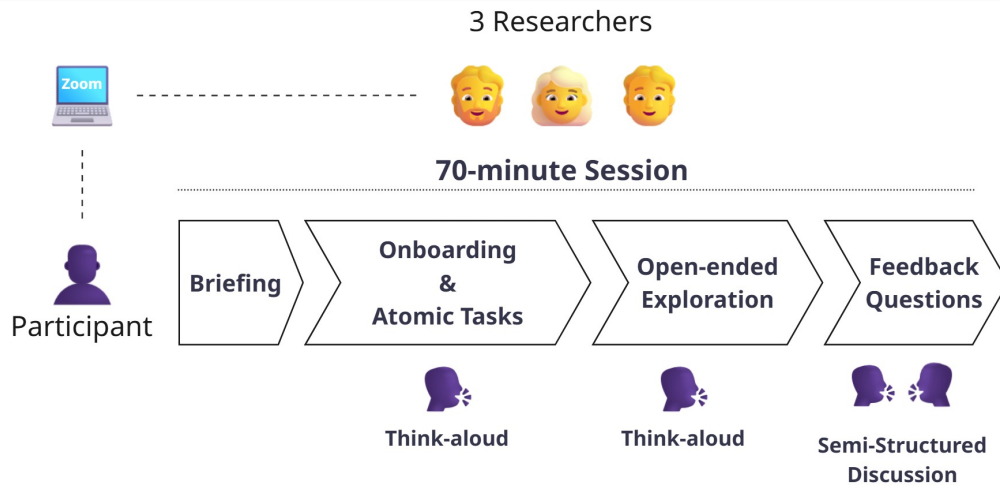


Figure 2. For the user study, participants took part in individual sessions, each lasting approximately 70 minutes and monitored by three researchers. Sessions were conducted via Zoom and structured into four stages. Both *Onboarding & Atomic Tasks* and *Open-ended Explorations* followed a think-aloud protocol. In contrast, *Feedback Questions* were conducted as a semi-structured discussion, guided by a set of predefined questions.

238 backtracking, minor or repetitive need for guidance, misunderstandings, or elements overlooked. Each
 239 observation was linked to a specific component where it occurred. To assess utility, we observed how the
 240 participant's reasoning relied on molIEReVIS during an open-ended exploration. We noted behaviors such
 241 as referring to visual cues, integrating information across multiple charts or stages, making comparisons,
 242 and attempting to identify patterns. Utility was also assessed through open-ended questions in which
 243 participants reflected on their experience and whether the system would be a helpful addition to their
 244 existing workflow. The session had the following structure:

- 245 1. Briefing and personal information: The participant was first briefed on the study's purpose and structure,
 246 and provided basic personal information.
- 247 2. Onboarding and atomic tasks: We decomposed each stage into independent sections. For each section,
 248 the participant first underwent a targeted onboarding. Then, the participant was asked to perform an
 249 atomic task focused on that specific section. These atomic tasks were designed to have a specific goal,
 250 so that it was clearly defined when a task was finished.
- 251 3. Open-ended exploration: The participant freely engaged with molIEReVIS in an open-ended
 252 exploration.
- 253 4. Feedback questions: The participant answered open-ended questions, offering feedback about
 254 molIEReVIS utility.

255 The study was conducted in online sessions via Zoom. For the onboarding parts, the researcher shared
 256 their screen with the participant, while during task completion and exploration, the participant shared
 257 their screen. We employed a think-aloud protocol during all sessions. Guidance was provided only when
 258 necessary or upon request. Figure 2 summarizes a session structure.

3 RESULTS

259 In this section, we present our results, including the design instantiation and the user study.

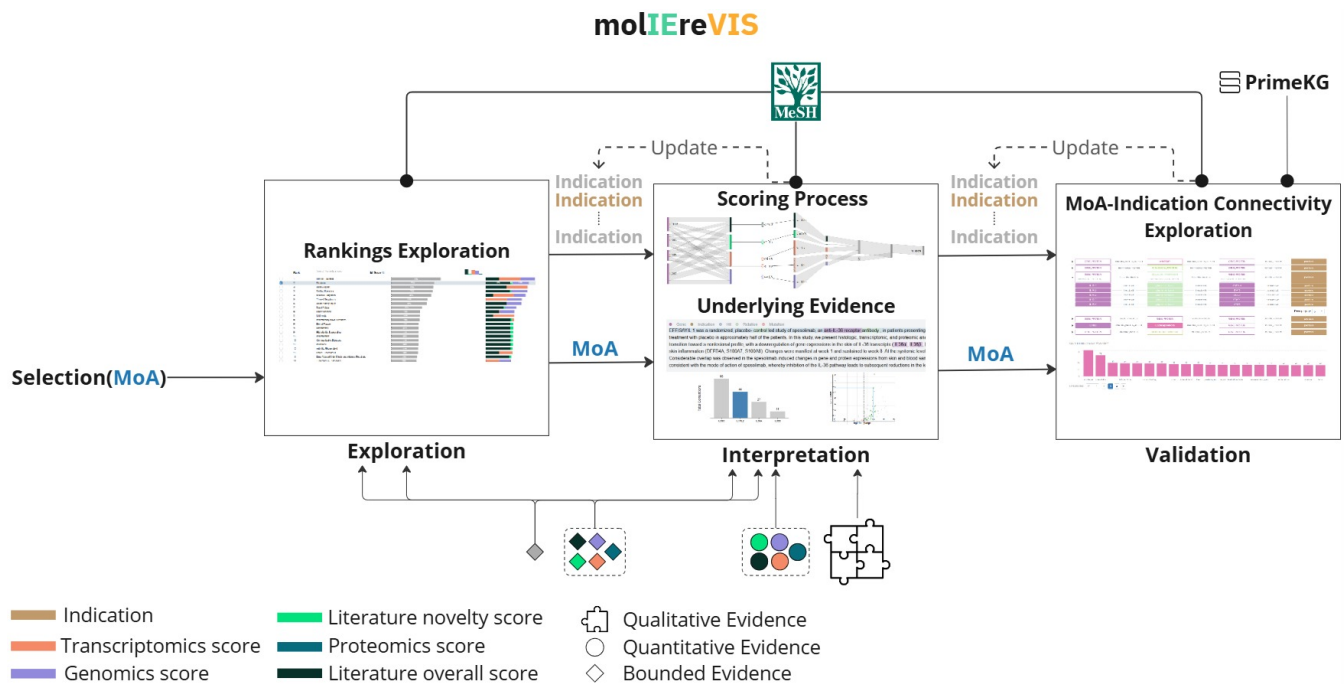


Figure 3. An overview of the designed multistage visualization workflow. The workflow starts by anchoring the analysis to a selected MoA. The user then narrows the focus to a specific indication, which can be updated at any time using the integrated MeSH disease ontology. The analysis proceeds through three stages: *Exploration*—molIERe’s results can be explored, visualizing both M_{score} and the bounded evidence produced by saturating the quantitative evidence; *Interpretation*—molIERe’s scoring process and its underlying evidence are revealed, visualizing both the quantitative and the qualitative evidence; *Validation*—an MoA–Indication connection of interest is validated by exploring established paths between the MoA and the corresponding disease in an independent knowledge graph.

260 3.1 Design Instantiation

261 In this section, we present molIEReVIS, our design instantiation. The implementation of molIEReVIS
 262 is tailored to molIERe, the operational pipeline for which it was developed. However, the visualization
 263 concepts adopted for the molIERe use case are adaptable to other pipelines, particularly those that
 264 explicitly realize all evidence transformation boundaries and quantify the collective evidence per stream in
 265 a scalar value. We discuss this adaptability in more detail in Section 4.4.

266 In alignment with DG1, we designed molIEReVIS as a three-stage workflow: exploration,
 267 interpretation, and validation (Figure 3). At the beginning of the analysis, the user is required to select an
 268 MoA of interest from a searchable list (DG2). In addition, the analysis is constrained to a specific indication
 269 of interest (DG2), which can be selected from either the ranking table or from a separate menu exposing
 270 the Medical Subject Headings (MeSH) disease ontology (U.S. National Library of Medicine, 2025) (DG6),
 271 which is widely used for literature indexing. We visualize the disease ontology as an interactive, expandable
 272 tree view (Figure 4), where users can explore level by level, with the ability to search. Each node in the tree
 273 is annotated with the consensus score from molIERe (M_{score}). For each node with children, the M_{score}
 274 distribution among descendant nodes spanning all levels down to the leaves is displayed in a dedicated
 275 column of sparklines. The resulting histograms highlight promising branches where high-ranked indications
 276 can be found.

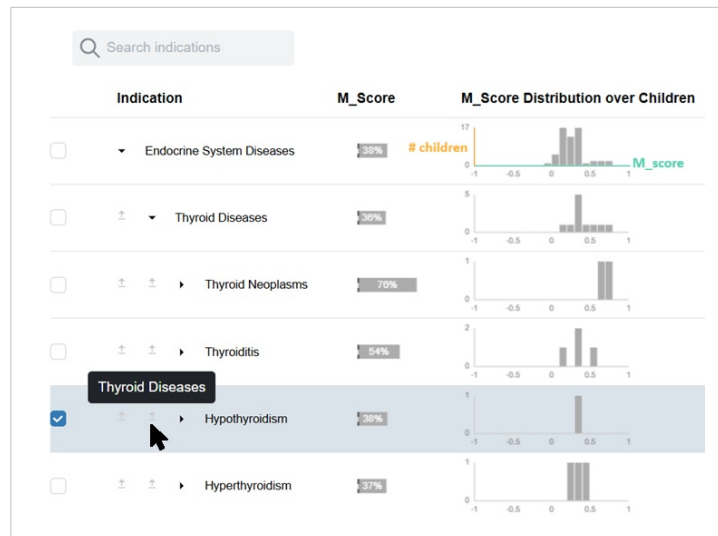


Figure 4. Users can select candidate indications of interest through the MeSH disease ontology, displayed as an expandable tree view. Each row represents a node in the ontology and can be expanded to reveal its child nodes. Every node is annotated with its corresponding M_{score} and a sparkline showing the distribution of M_{score} across its descendant nodes down to the leaves. On-demand hints associated with indentation levels help users easily identify parent–child relationships, even when nodes are expanded far from their parents.

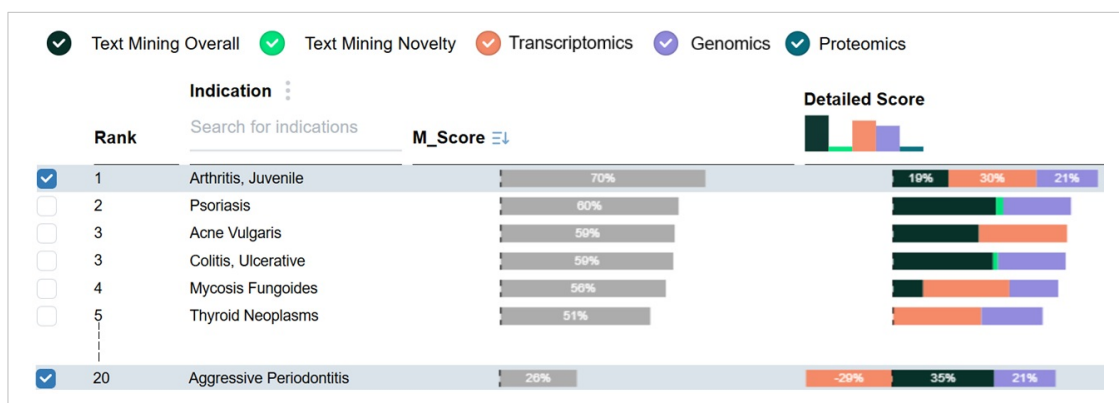


Figure 5. Indication ranking table displaying M_{score} column and *Detailed score* column breaking down the consensus score into contributions from individual data streams. The twentieth indication shows the visual encoding for the negative contribution from the transcriptomics data stream.

277 In the following subsections, we outline our design for the different stages in molIEreVIS, including
 278 the basic interaction with the visual elements.

279 3.1.1 Exploration Stage

280 For the ranking list visualization, we adapt the visualization technique proposed in LineUp (Gratzl et al.,
 281 2013), designed to represent rankings based on heterogeneous attributes. LineUp adopts a column-based
 282 view in which each column corresponds to an attribute, with its values visualized as bar charts. Multiple
 283 attributes can be combined using a weighted sum by dragging and dropping their columns, and the resulting
 284 score is shown as a stacked bar chart.

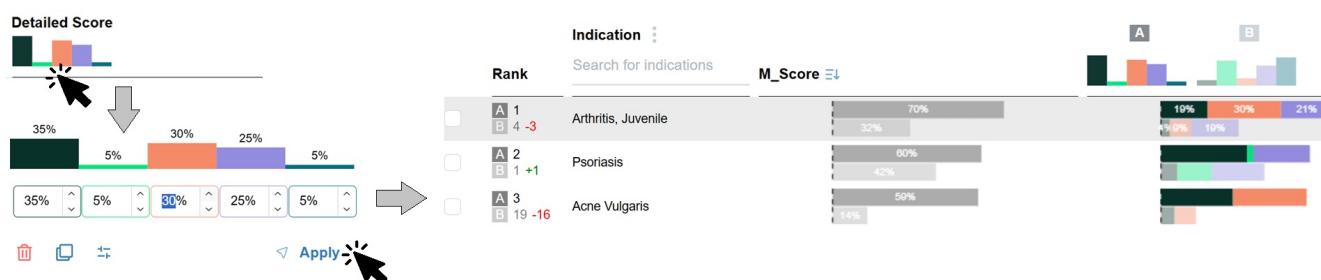


Figure 6. Clicking the weight bar chart in the *Detailed score* header opens a pop-up dropdown that allows users to adjust existing weights, add new ones, and select a weight set as a reference for ranking comparison. Each newly defined weight set generates an additional M_{score} bar chart alongside the default ones in the ranking table, enabling direct observations for weight influence.

285 A key distinction in our data compared to typical LineUp use cases is the presence of negative attribute
 286 values, which represent opposing evidence. To handle this, our bar charts use a zero pivot, with negative
 287 values extending to the left.

288 We limited the visualization and interactivity offered in LineUp to keep our visualization focused and
 289 task-oriented. We describe our design for the ranking table in the following points:

- 290 • M_{score} column: A bar chart column showing M_{score} .
- 291 • *Detailed score* column: A stacked bar chart column to break down M_{score} by data stream contribution.
- 292 • *Data stream toggling*: An option for the user to selectively toggle data streams on or off, thereby
 293 adjusting those that govern the rankings (DG5).

294 Figure 5 shows the ranking table for *anti-IL1RL2*, which is a known MoA for the treatment of *Psoriasis*.
 295 Consistent with domain knowledge, *Psoriasis* appears among the top candidate indications.

296 The stage also allows users to adjust data stream weights and observe their impact on the rankings (DG5).
 297 As shown in Figure 6, users can add a new set of weights by interacting with the weights bar chart in the
 298 *Detailed score* header. A pop-up drop-down appears, allowing weight values to be entered directly into text
 299 boxes. Each weight set is visualized as a shaded bar chart in the header and is labeled with a letter for easy
 300 reference. Up to five sets of weights can be added

301 When a new weight set is added, a new M_{score} is calculated for each indication. These are displayed as
 302 shaded bars and stacked bars in the ranking table. Each additional bar is aligned with the corresponding
 303 weight set letter label in the *rank* column, which also visually encodes ranking changes as numerical green
 304 annotation for increases, and red for decreases.

305 3.1.2 Interpretation Stage

306 In line with DG1 and DG3, we designed the **evidence-flow diagram** shown in Figure 7. It consists of
 307 several layers arranged from left to right, comprised of nodes with links between them tracing evidence
 308 across its transformation boundaries realized by molIERe (see Figure 1).

309 Each node in layer 1 belongs to a molecular target of the MoA of interest, and each node in layer 2
 310 represents the collective qualitative evidence of a data stream. The extent of hatching on a node reflects the
 311 presence of opposing evidence. Up to layer 2, the evidence collected from different data streams is not
 312 yet harmonized and therefore not comparable. For this reason, we treat the data stream nodes in layer 2
 313 independently, giving each the same fixed size. Meanwhile, the links between the two layers represent how

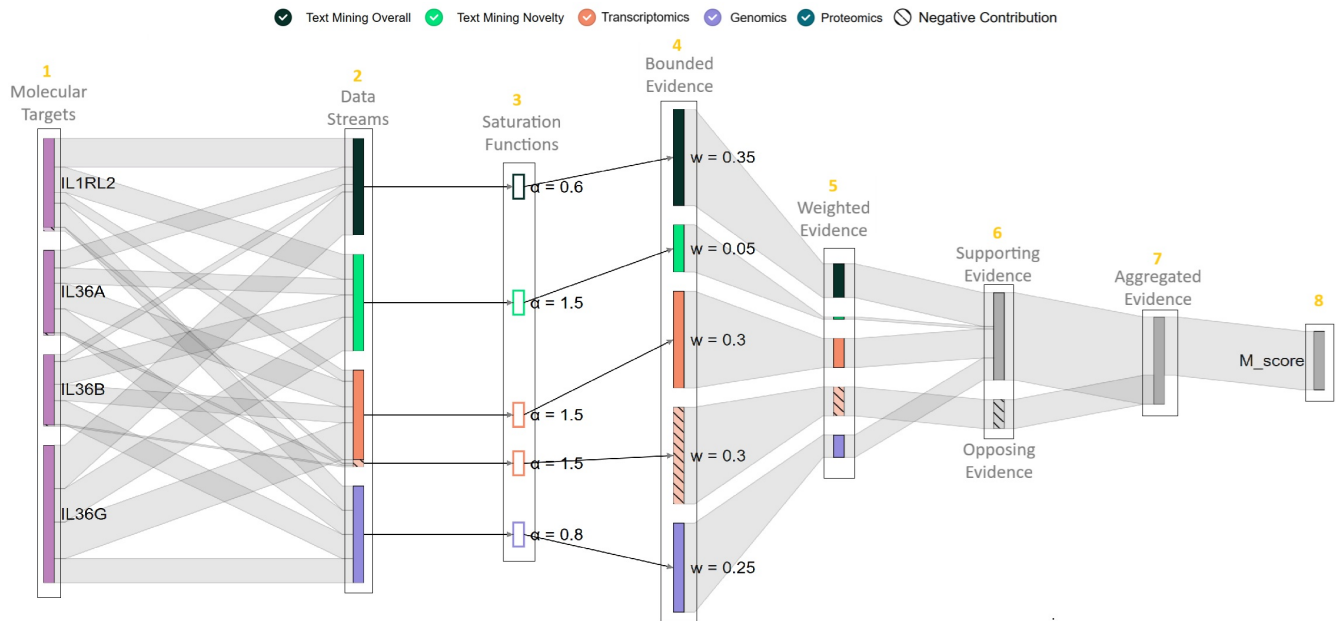


Figure 7. The **evidence flow diagram** designed for tracing the evidence during the M_{score} calculation process. The diagram consists of layers with nodes and links between nodes that trace the flow and transformation of evidence across layers. It also exposes the weight and saturation parameters queried by the molIEReVIS backend from the PostgreSQL database. The figure shows the diagram for the association between *anti-IL1RL2* and *Psoriasis*.

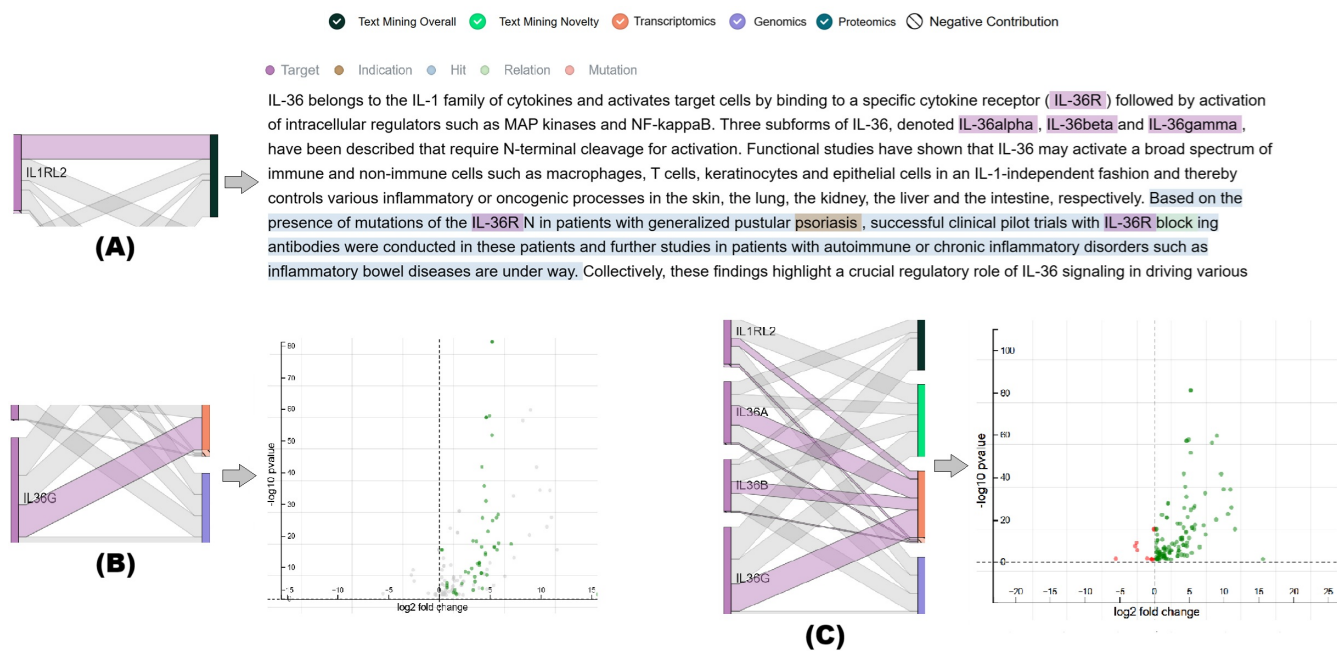


Figure 8. By interacting with the links between the target and data stream layers in the evidence flow diagram, users can drill down into the detailed qualitative evidence underlying the M_{score} calculation. The figure shows several pieces of evidence for the association between *anti-IL1RL2* and *Psoriasis*. (A) An abstract retrieved by the text mining algorithm. Highlighted segments indicate the different aspects considered supporting the association by the algorithm and relevant to the *IL1RL2* receptor. (B) A volcano plot highlighting the parts of the transcriptomics evidence associated with the *IL36G* ligand. (C) Volcano plot with all the transcriptomics evidence highlighted due to selecting all links to the MoA targets.

314 the total normalized evidence collected by each data stream is distributed among the targets. Consequently,
315 the target node size represents the aggregated normalized support it receives across data streams.

316 Layer 3 shows the different saturation functions applied to the evidence based on its source. After
317 saturation, layer 4 corresponds to the harmonized evidence, where the size of the node represents its
318 bounded value. Subsequently, evidence integration starts at layer 5, the harmonized evidence is scaled
319 by a weight corresponding to each data stream. We group the supporting evidence versus the opposing
320 evidence in layer 6, then we aggregate them in layer 7. The intersection between the supporting and
321 opposing links flowing from layer 6 to layer 7 shows the amount of the decreased support reduced by the
322 opposing evidence. Finally, layer 8 represents the produced M_{score} and whether it is toward or against the
323 new MoA–indication association.

324 As an example of the insights that can be derived from tracing the evidence transformation in this diagram,
325 Figure 7 shows the diagram for the association between *anti-IL1RL2* and *Psoriasis*. The opposing portion of
326 the transcriptomic evidence seems to balance the positive one, which leads to a nearly neutral contribution
327 to the consensus score by this data stream. However, layer 2 shows that the actual amount of opposing
328 evidence is small compared to the supporting one, indicating that the harmonization process skews the
329 relative contributions of the positive and negative parts.

330 For enhanced traceability of the evidence, the diagram displays the exact scalar value of the transformed
331 evidence when hovering over the nodes in each layer. In addition, selecting a saturation function node in
332 layer 3 plots the corresponding function for the specific data stream. To fully satisfy **DG3**, inline with
333 **DG1** we enable evidence drill-down-analysis. Selecting the links between layer 1 and layer 2 enables users
334 to drill down into a summary visualization of the collective qualitative evidence. For example, selecting
335 the link between *IL36G* and the transcriptomics stream node displays a volcano plot presenting the full
336 transcriptomics evidence, with the pieces corresponding to *IL36G* highlighted (see Figure 8 (B)).

337 Furthermore, selecting a piece of the visualized collective evidence enables users to drill down to its
338 corresponding qualitative representation. For example, Figure 8 (A) shows the abstract of a selected
339 publication analyzed by the text-mining algorithm. As illustrated in the same figure, at this level of
340 analysis, we can also provide an instance-level explanation: the abstract is highlighted according to the
341 specific aspects identified by the text-mining algorithm to support *anti-IL1RL2–Psoriasis* association.
342 molIEreVIS highlights the abstract using annotation data generated by the text-mining algorithm itself.

343 3.1.3 Validation Stage

344 This stage functions as a consistency validation, allowing users to assess whether the MoA-disease
345 association is compatible with broader existing curated knowledge, thereby addressing **DG4**. To this end, we
346 employ PrimeKG (Chandak et al., 2023), a comprehensive knowledge graph that, at the time of publication,
347 integrates 20 high-quality resources to describe 17,080 diseases with 4,050,249 relationships. It represents
348 ten major biological scales including disease-associated protein perturbations, biological processes and
349 pathways, anatomical and phenotypic scale, and the entire range of approved and experimental drugs with
350 their therapeutic action. PrimeKG inevitably reflects existing literature biases. However, because this stage
351 operates within a human-in-the-loop workflow rather than as an automated decision rule, such biases can
352 be consciously accounted for by experts. For example, underrepresentation of first-in-class MoA would
353 not lead to outright rejection of a candidate, but could instead be interpreted as a potential gap in current
354 knowledge.



Figure 9. (A) A sample query and several of the retrieved meta-paths. The number of actual paths grouped under each meta-path is shown on its right end. (B) An example of an expanded meta-path, showing the paginated grouped paths and the filter input available for each type node. (C) A paginated distribution chart summarizing the contribution of different anatomies to the paths grouped under a single meta-path. Hovering over the bar displays the entity name and its count.

355 Inspired by previous work (Wang et al., 2022; Nunes and Pesquita, 2024; Jiang et al., 2025), we chose
 356 a *path-based representation* for the MoA–indication connectivity: we display independent sequences
 357 of entities connecting the MoA to the indication, rather than showing a full *node-link diagram*. These
 358 sequences are subgraphs that connect an MoA linearly with an indication via intermediate nodes. We chose
 359 this design because the path-based representation aligns more closely with experts’ mental models and
 360 the way they communicate their findings, which was also noted by Wang et al. (2022) who empirically
 361 demonstrated its efficiency compared to the node-link diagram.

362 We designed this stage as a query interface for PrimeKG. The user can build two-sided queries: the left
 363 side represents a selected MoA, and the right side represents an indication to validate. The query retrieves
 364 the shortest paths between the two sides. Since PrimeKG does not include MoA nodes directly, we use the
 365 molecular targets of the MoA as the left side of the query. The user can optionally exclude any of these
 366 targets from their query.

367 We represent query results as *meta-paths*. A meta-path is a sequence of node and edge types that groups
 368 semantically similar paths. In line with **DG1**, our meta-paths are expandable. When expanded, a meta-path
 369 reveals the paths with actual entities and links in PrimeKG that follow its structural pattern. Because the
 370 number of such paths can be large, we paginate them and allow users to optionally define the page size. In
 371 line with Wang et al. (2022), we visually distinguish between a *type node* (nodes that represent a type of
 372 entity, such as protein or anatomy) in a meta-path and an actual *entity node*, by representing type nodes as
 373 outlined rectangles and entity nodes as filled rectangles. Each of the 20 node types in PrimeKG is assigned
 374 a unique color. Type nodes in meta-paths provide filters that enable users to sharpen their exploration,

375 focusing on a subset of the grouped paths. Meta-paths are displayed in descending order based on the
376 number of paths they group, and users have the option to change this order.

377 Figure 9 (A) illustrates a query for paths connecting *anti-IL1RL2* with *Psoriasis*, and several of the
378 retrieved meta-paths. Figure 9 (B) illustrates an expanded meta-path showing how *IL1RL2*, *IL36G*, and
379 *IL36B* interact with the *Interleukin-36* pathway, a pro-inflammatory signaling cascade implicated in
380 psoriasis. This meta-path supports the role of *IL1RL2* as the receptor mediating *IL-36*-driven inflammatory
381 responses in psoriatic pathology. In addition, as shown in Figure 9 (C), when a type node in a meta-path
382 is selected, molIEreVIS displays a distribution chart that summarizes the PrimeKG entities grouped
383 under this type node. For example, the distribution chart in Figure 9 (C) reveals that esophagus is the most
384 prevalent anatomy entity in this meta-path.

385 3.2 User Study Results

386 In this section, first, we highlight the usability difficulties we observed in the current design. Second, we
387 summarize our observations during the open-ended exploration. Finally, we present the feedback collected
388 from the post-study open-ended questions.

389 3.2.1 Usability difficulties

390 Most of the hesitation was observed in the exploration stage, in particular during the atomic tasks when
391 participants engaged with the weight comparison interface. Participants either forgot a required step for
392 completing the interaction, triggering an intervention on our side, or became confused for a moment when
393 adding a new weight set, adjusting it, or making it the reference set. In contrast, during the open-ended
394 task, participants overcame their hesitation and interacted more smoothly with the interface. This pattern
395 suggests that while the current design is ultimately learnable, it is not immediately intuitive and would
396 benefit from improved procedural clarity. In addition, all participants overlooked indications sharing
397 the same rank in the ranking table, suggesting a need for a visual encoding to make this situation more
398 perceptible. Some difficulty was also observed in the engagement with the MeSH ontology. In particular,
399 **P3**, who is least familiar with the molIEre pipeline processes, hesitated when asked how to incorporate
400 the M_{score} distribution sparklines in their analysis. Participants **P1** and **P2** interacted more smoothly with
401 this interface, and **P2** stated “*The distribution histogram is helpful to quickly get an idea of which disease*
402 *groups to check out further*”. The only usability issue we observed during the validation stage was that
403 participants found it tedious to deselect the irrelevant disease names suggested by the fuzzy matching. No
404 noteworthy usability difficulties were observed during the interpretation stage.

405 3.2.2 Open-ended exploration

406 Overall, all three participants demonstrated a clear understanding of the workflow after completing the
407 onboarding and atomic tasks. They were able to interact smoothly and meaningfully with molIEreVIS,
408 interpret its visual cues, obtain insights, and integrate information across the different stages to assess
409 plausible indications. During the open-ended exploration, the exploration stage proved to be a good entry
410 point for the analysis. Participants found it to be integrated well with the following stages, and to align with
411 their typical assessment workflow. One participant found the original indication for an MoA among its
412 top-ranked indications, stating “*That’s a good sign! I’m happy with the rankings*” (**P2**). **P3** looked for one
413 indication they had in mind in the ranking table, which turned out to have a low rank and lack evidence.
414 Upon checking the validation stage, the participant found the paths relatively long and characterized by
415 negative relationships, and commented “*I’m not surprised*” (**P3**).

416 Interestingly, participants spent most of their open-ended exploration time in the interpretation stage. All
417 participants drilled down to the underlying evidence and appreciated the integrated access to the diverse
418 data sources, especially the convenient access to publications and their abstracts collected through the
419 text mining stream. All participants also liked the highlighted segments in the abstracts that indicate the
420 different aspects considered by the text mining algorithm. **P1** appreciated the visual clarity of the evidence
421 flow diagram in distinguishing supporting from opposing evidence, a distinction that she described as
422 “harder to see in our deep dives”. **P1** wanted to compare the evidence flow diagram and its underlying
423 evidence for two indications. As our current design does not support direct comparison, she moved back
424 and forth between evidence charts for two indications, observing that “This indication is supported by
425 more publications, but the other seems to be supported by more novel ones” (**P1**). She expressed interest in
426 facilitating the comparison: “I’d have liked more comparison features” (**P1**).

427 In the validation stage, **P1** was surprised to find only one path connecting the selected MoA and the
428 candidate indication, but stated: “Interesting to look at this path, I would definitely have missed this” (**P1**).
429 **P2** explained her reasoning for examining the paths: “The length of the paths and intermediate nodes can
430 tell you how well something is studied” (**P2**). Across participants, we observed a strong reliance on the
431 distribution charts to identify dominant biomedical entities under a node type, which they preferred over
432 using the filtering feature. While **P1** and **P2** expressed enthusiasm about further exploring the validation
433 stage, both **P1** and **P3** felt that this stage was overloaded with information. Additionally, **P3** expressed
434 interest in being able to construct more flexible queries within this stage.

435 3.2.3 Feedback

436 All participants agreed that molIEreVIS would be a valuable addition to their typical workflow, by
437 enabling rapid identification of promising indications for further investigation: “Quick checks can be easily
438 performed for indications” (**P1**). They also reported feeling well supported in their analyses, particularly
439 when leveraging the interpretation stage. **P2** suggested two additional extensions that would make her feel
440 even more supported: the ability to combine and export multiple visualizations into a compact “disease
441 card” summarizing findings for a given indication, and the incorporation of LLMs to generate summaries
442 of the evidence.

4 DISCUSSION

443 In this section we reflect on learnings from the user study and derive interesting avenues for future work
444 from our findings.

445 4.1 Ranking List and MeSH Interface

446 Overall, molIEreVIS was well received by our small group participants. However, as described in
447 Section 3.2.1, we also noticed some parts of the workflow that could have been smoother. In particular, we
448 were surprised that the exploration stage seemed to cause the most confusion. Being based on a simple
449 ranking table and a selection interface using the MeSH disease ontology, we deemed this stage the most
450 straightforward in terms of usability. During the user study, we identified two potential improvements.

451 One, users got confused by the discrepancy between the ranking table and the MeSH tree. The ranking
452 table lists only terms for which the pipeline had been run, and the terms are presented in a flat list. Here,
453 items appear flush left regardless of the level at which they would appear in the MeSH hierarchy. In contrast,
454 in the MeSH tree view, all MeSH terms are present, but the ones for which no pipeline data is available
455 cannot be selected. A future version of molIEreVIS could attempt to incorporate the MeSH hierarchy

456 directly in the ranking. We considered such an approach during the design phase, but ultimately decided to
457 split the interaction between the simpler, flat table and the dedicated MeSH view.

458 Two, the modification of weights and the comparison of rankings caused some confusion. While we
459 attribute this in part to some of the participants not being familiar with molIEre processes, we are
460 still trying to understand how the UI could be improved to better support this task. Ranking comparison
461 involves the creation of a new set of weights, the definition of a reference set of weights, and understanding
462 the visualized ranking differences. To improve this workflow, we originally considered the introduction
463 of bump charts to more explicitly encode ranking changes, but found them to clash with the compact
464 horizontal stacking of the M_{score} charts. We chose this stacking in the first place due to its suitability for
465 comparison. It remains a challenge to find a more intuitive workflow for the ranking comparison task in
466 molIEreVIS—even though it must be noted that we expect a limited number of users to often experiment
467 with different weights.

468 4.2 Evidence Flow Chart

469 We were delighted by how intuitively all users interacted with it, even though it included several custom
470 encodings that users could not have been familiar with from other tools. In particular, the changing
471 node scale throughout the pipeline steps and the encoding of negative values, which typically cannot be
472 represented in standard Sankey charts, did not confuse any of the study participants.

473 Still, one of the takeaways from the user study concerns the evidence flow chart and its use in the
474 interpretation stage. As stated in Section 3.2.2, one participant mentioned that they would have liked better
475 comparison features during this stage. With the current design, a comparison of two diseases for the same
476 MoA could be achieved by placing the molecular target nodes at the center and having two copies of
477 the chart—one for each disease—fanning out to either side. To further facilitate comparison, it might be
478 necessary to allow users to collapse parts of the chart to bring nodes and edges to be compared closer
479 together. A dedicated comparison would also require a vertical alignment of nodes across diseases. It is
480 not obvious how the current design can be directly used for comparing more than two diseases, other than
481 simply juxtaposing multiple linked evidence charts.

482 4.3 Path Exploration

483 Our participants felt overwhelmed by the amount of information shown during the validation stage. We
484 attribute this observation to the fact that the participant's current workflow is not based on paths through a
485 dense knowledge graph like PrimeKG. Moreover, in some cases, many hundreds or thousands of “shortest”
486 paths can exist, with dozens of different meta-paths. In those cases, it might be beneficial not to show all
487 available information but to introduce further abstraction layers. These abstraction layers can take the form
488 of visual summaries, each conveying a specific aspect of all paths instantiated by a given meta-path. Such
489 representations enable users to reason about the global structure before drilling down into individual paths.
490 For example, an under-planning representation visualizes a meta-path as a conditional relationship between
491 entity sets defined by the query endpoints, for instance the relationship between the set of disease-associated
492 genes and the set of anatomical contexts in which a gene is expressed.

493 The recent work by Jiang et al. (2025) demonstrates how LLMs, when combined with knowledge graphs,
494 can assist experts in iteratively exploring, reasoning about, and refining hypotheses derived from complex
495 knowledge graph paths. Incorporating LLMs could also be a promising direction in molIEreVIS to
496 mitigate information overload. In a related research project on knowledge graph curation, we gained
497 positive experience with a customized LLM chat that has access to the selections and encodings of a visual

498 interactive tool. However, it is crucial to keep the interaction between the LLM and the user collaborative
499 rather than fully autonomous to maintain reliability and prevent hallucination.

500 In addition, inspired by Partl et al. (2016), we are already developing an improved visual query editor
501 that allows users to flexibly filter the paths shown, which should improve the process of finding individual
502 paths or groups of paths of interest, even when there are many meta-paths.

503 4.4 Different Data Contexts and Additional Data Streams

504 The visualization approach resulting from this study is grounded in a conceptual model of multimodal
505 drug repurposing pipelines (see Table 3). This abstraction enhances adaptability in different data, and
506 pipeline contexts beyond the specific instantiation demonstrated in this paper. In this section, we discuss
507 this adaptability in more detail.

508 As for the implementation scope specific to the context of molIEre, the demonstrated components of
509 molIEreVIS are modular and can be substituted as needed. For instance, although we use PrimeKG in
510 the validation stage, any knowledge graph can be used instead. The same flexibility applies to the choice of
511 disease ontology that, in our demonstration, is MeSH. Moreover, additional data streams can, in principle,
512 be integrated into the workflow. In practice, a new data stream requires the development of corresponding
513 collective and individual piece of evidence charts, that will be shown when a link corresponding to evidence
514 of the newly added data modality is selected in the evidence flow chart. In terms of visual scalability, we
515 expect the evidence flow chart to easily scale to about twice as many data streams as are implemented in
516 the prototype version.

517 As discussed in Section 2.2, beyond molIEre different pipelines may realize evidence transformation
518 boundaries in different ways. In particular, some multimodal pipelines collapse multiple boundaries by
519 embedding heterogeneous evidence into a shared latent representation and performing evidence integration
520 within a single black-box model. In such cases, the intermediate data artifacts associated with the collapsed
521 boundaries are no longer explicitly available. Accordingly, DG3 reflects an intentional abstraction that
522 avoids exposing these collapsed data artifacts, namely low-level model states, which would not align with
523 the target users' understanding of the pipeline or their reasoning model.

524 The integration boundary is essential for the multimodal drug repurposing pipelines. However, some
525 pipelines may not explicitly expose per-stream contributions. In such cases, DG3 recommends estimating
526 these contributions, as they constitute an important data artifact in expert reasoning model. One way to
527 restore the interpretability can be by computing feature attributions with established methods and grouping
528 them by evidence stream.

529 Additionally, the instance-level explanations used for the literature-based evidence stream in
530 molIEreVIS can be understood more generally as a drill-down mechanism for evidence investigation. In
531 pipelines where evidence is transformed using model-based approaches, a comparable visualization could
532 be supported through established attribution methods that relate model outputs back to individual evidence
533 instances.

534 “What-if” analysis DG5 remains feasible in collapsed-boundary settings by operating at the level of
535 evidence rather than model internals. Such analysis can be enabled by perturbing semantically meaningful
536 groups of input evidence (e.g., entire data streams or subsets), for example by selectively removing,
537 substituting, or reweighting them. This allows users to explore alternative scenarios and assess the
538 robustness of results without requiring direct control over the collapsed transformation boundaries.

539 Finally, although this work primarily addresses decision support for drug repurposing, as noted in Section
540 2.2, the conceptual model of multimodal pipelines on which our study is grounded has also been observed
541 in other drug discovery domains, such as target prioritization and biomarker discovery. These domains
542 serve as potential directions for extending the adaptability of this study.

543 4.5 Additional Features

544 In our open discussions toward the end of the user study sessions, participants mentioned two concrete
545 ideas for future extensions of molIereVIS.

546 One, experts sometimes prepare so-called disease cards to present and document the findings of the
547 assessment process in a compact form. It should be relatively straightforward to include a mechanism for
548 exporting selected charts or publication details for use in such disease cards. However, it is not clear how to
549 merge the findings from molIereVIS efficiently with evidence users might have found elsewhere. This
550 might be necessary because users mentioned that they found it likely to incorporate molIereVIS in their
551 workflows, but that they do not want to completely abandon their existing practices in its favor.

552 Two, users commented that they would appreciate automatic textual summaries of evidence directly
553 within molIereVIS. In the future, we would like to experiment with LLM-based summaries (Xu et al.,
554 2024; Choi et al., 2025) of the various charts, in particular, the summary plots accessible through the
555 evidence flow chart. The text-mining evidence may also serve as a rich source for textual summarization.

556 While we are eager to explore this further, we realize the risk of hallucinations in the context of evidence
557 analysis. Therefore, the expert should remain the final decision maker, using the LLM output as contextual
558 guidance rather than authoritative conclusions.

559 5 CONCLUSION

560 In this paper, we presented an interactive visualization approach designed to support experts in
561 evaluating drug repurposing opportunities prioritized by a computational pipeline that integrates evidence
562 from multimodal data sources. Grounded in a design study, our approach abstracts domain experts'
563 practices into a staged reasoning workflow comprising exploration, interpretation, and validation. We
564 also demonstrated molIereVIS, which instantiates our approach within an operational multimodal
565 drug repurposing pipeline. molIereVIS exposes candidate rankings, evidence provenance across
566 transformation boundaries, and knowledge graph context in a coordinated manner. Experts' feedback on
567 molIereVIS highlights the potential for improving computational drug repurposing workflows through
568 interactive visualization.

569 ACKNOWLEDGMENTS

570 This work was partly supported by Boehringer Ingelheim RCV GmbH & Co KG, the Austrian Science
571 Fund (FWF DFH 23-N), and the Austrian Research Promotion Agency (FFG 911655: "Pro²Future").

572 We used OpenAI's ChatGPT (GPT-3 to GPT-5.1) large language models accessed via [https://](https://chatgpt.com/)
573 chatgpt.com/ and Grammarly accessed via the Chrome extension [https://www.grammarly.](https://www.grammarly.com/browser/chrome)
574 [com/browser/chrome](https://www.grammarly.com/browser/chrome) as a writing assistant. The tools were used in an iterative human-in-the-loop
575 manner to suggest rephrasings and improve grammar and structure, similar to a rubber-duck debugging
576 process for prose. AI-generated text was critically reviewed, edited, and rewritten by the authors. No
577 generative AI tools were used to create or modify data or figures.

REFERENCES

- 576 Adamek, L., Padiasek, G., Zhang, C., O'Dwyer, I., Capit, N., Dormont, F., et al. (2024). Identifying
577 indications for novel drugs using electronic health records. *Computers in Biology and Medicine* 183,
578 109158
- 579 Ashburn, T. T. and Thor, K. B. (2004). Drug repositioning: identifying and developing new uses for
580 existing drugs. *Nature reviews Drug discovery* 3, 673–683
- 581 Brown, A. S. and Patel, C. J. (2018). A review of validation strategies for computational drug repositioning.
582 *Briefings in bioinformatics* 19, 174–177
- 583 Cavalla, D. (2019). Using human experience to identify drug repurposing opportunities: theory and practice.
584 *British Journal of Clinical Pharmacology* 85, 680–689
- 585 Chandak, P., Huang, K., and Zitnik, M. (2023). Building a knowledge graph to enable precision medicine.
586 *Scientific Data* 10, 67
- 587 Choi, R., Burns, F., and Lawrence, C. (2025). End-to-end chart summarization via visual chain-of-thought
588 in vision-language models. *arXiv preprint arXiv:2502.17589*
- 589 Cousins, H. C., Nayar, G., and Altman, R. B. (2024). Computational approaches to drug repurposing:
590 methods, challenges, and opportunities. *Annual Review of Biomedical Data Science* 7
- 591 Cremin, C. J., Dash, S., and Huang, X. (2022). Big data: Historic advances and emerging trends in
592 biomedical research. *Current Research in Biotechnology* 4, 138–151. doi:[https://doi.org/10.1016/j.crbiot.
593 2022.02.004](https://doi.org/10.1016/j.crbiot.2022.02.004)
- 594 Gratzl, S., Lex, A., Gehlenborg, N., Pfister, H., and Streit, M. (2013). Lineup: Visual analysis of
595 multi-attribute rankings. *IEEE transactions on visualization and computer graphics* 19, 2277–2286
- 596 Gurbuz, O., Alanis-Lobato, G., Picart-Armada, S., Sun, M., Haslinger, C., Lawless, N., et al. (2022).
597 Knowledge graphs for indication expansion: an explainable target-disease prediction method. *Frontiers
598 in genetics* 13, 814093
- 599 Hamid, A., Mäser, P., and Mahmoud, A. B. (2024). Drug repurposing in the chemotherapy of infectious
600 diseases. *Molecules* 29, 635
- 601 Henry, S. and McInnes, B. T. (2017). Literature based discovery: models, methods, and trends. *Journal of
602 biomedical informatics* 74, 20–32
- 603 Hill, R. G. and Richards, D. (2021). *Drug discovery and development: technology in transition* (Elsevier)
- 604 Huang, K., Chandak, P., Wang, Q., Havaladar, S., Vaid, A., Leskovec, J., et al. (2024). A foundation model
605 for clinician-centered drug repurposing. *Nature Medicine* 30, 3601–3613
- 606 Iqbal, M. W., Sun, X., Sasidharan, R. S., Haider, S. Z., Al-Ghanim, K. A., Nawaz, M. Z., et al. (2025).
607 Integrative machine learning and structure-based drug repurposing for identifying potent inhibitors of
608 human syk activity against cancer. *Life Sciences* , 123814
- 609 Ivanisevic, T. and Sewduth, R. N. (2023). Multi-omics integration for the design of novel therapies and the
610 identification of novel biomarkers. *Proteomes* 11, 34
- 611 Jarada, T. N., Rokne, J. G., and Alhajj, R. (2020). A review of computational drug repositioning: strategies,
612 approaches, opportunities, challenges, and directions. *Journal of cheminformatics* 12, 46
- 613 Jiang, H., Shi, S., Yao, Y., Jiang, C., and Li, Q. (2025). Hypochainer: a collaborative system combining llms
614 and knowledge graphs for hypothesis-driven scientific discovery. *IEEE Transactions on Visualization
615 and Computer Graphics* , 1–11doi:10.1109/TVCG.2025.3633887
- 616 Jiménez, A., Merino, M. J., Parras, J., and Zazo, S. (2024). Explainable drug repurposing via path based
617 knowledge graph completion. *Scientific Reports* 14, 16587

- 618 Khan, M. S., Shamsi, A., Zuberi, A., and Shahwan, M. (2025). In silico repurposing of fda-approved drugs
619 against MEK1: structural and dynamic insights into lung cancer therapeutics. *Frontiers in Pharmacology*
620 Volume 16 - 2025. doi:10.3389/fphar.2025.1619639
- 621 Kulkarni, V., Alagarsamy, V., Solomon, V., Jose, P., and Murugesan, S. (2023). Drug repurposing: an
622 effective tool in modern drug discovery. *Russian journal of bioorganic chemistry* 49, 157–166
- 623 Li, Z. and Ke, Z. (2025). RepoLLM: A multi-modal foundation model for drug repurposing via alignment
624 of molecules, EHRs, and knowledge graphs. In *ICML 2025 Workshop on Multi-modal Foundation*
625 *Models and Large Language Models for Life Sciences*. 8 pages
- 626 Liu, Z., Fang, H., Reagan, K., Xu, X., Mendrick, D. L., Slikker Jr, W., et al. (2013). In silico drug
627 repositioning—what we need to know. *Drug discovery today* 18, 110–115
- 628 López de Maturana, E., Alonso, L., Alarcón, P., Martín-Antoniano, I. A., Pineda, S., Piorno, L., et al.
629 (2019). Challenges in the integration of omics and non-omics data. *Genes* 10, 238
- 630 Lv, X., Wang, J., Yuan, Y., Pan, L., Liu, Q., and Guo, J. (2024). In silico drug repurposing pipeline using
631 deep learning and structure based approaches in epilepsy. *Scientific Reports* 14, 16562
- 632 March-Vila, E., Pinzi, L., Sturm, N., Tinivella, A., Engkvist, O., Chen, H., et al. (2017). On the integration
633 of in silico drug design methods for drug repurposing. *Frontiers in pharmacology* 8, 272508
- 634 McDonagh, E. M., Trynka, G., McCarthy, M., Holzinger, E. R., Khader, S., Nakic, N., et al. (2024).
635 Human genetics and genomics for drug target identification and prioritization: Open targets’ perspective.
636 *Annual review of biomedical data science* 7, 59–81
- 637 Ngernsombat, C., Suriya, U., Prattapong, P., Verma, K., Rungrotmongkol, T., Soonkum, T., et al. (2024).
638 Repurposing fda-approved drugs targeting fzd10 in nasopharyngeal carcinoma: insights from molecular
639 dynamics simulations and experimental validation. *Scientific reports* 14, 31461
- 640 Nielsen, J. (2012). Usability 101: Introduction to usability. Accessed: 2025-04-08
- 641 Nikolakis, D., Li Yim, A. Y., Overberg, K. L., Ghiboub, M., Wildenberg, M. E., de Jonge, W. J., et al.
642 (2025). Drug repurposing approach for the discovery of therapeutic agents for crohn’s disease-associated
643 intestinal fibrosis. *Journal of Crohn’s and Colitis* , jjaf137
- 644 Nunes, S. and Pesquita, C. (2024). Drug repurposing hypothesis validation with knowledge-infused
645 explanations. In *CEUR Workshop Proceedings (CEUR-WS)*, vol. 3833, article no. 2
- 646 Ozery-Flato, M., Goldschmidt, Y., Shaham, O., Ravid, S., and Yanover, C. (2020). Framework for
647 identifying drug repurposing candidates from observational healthcare data. *Jamia Open* 3, 536–544
- 648 Parisi, D., Adasme, M. F., Sveshnikova, A., Bolz, S. N., Moreau, Y., and Schroeder, M. (2020). Drug
649 repositioning or target repositioning: A structural perspective of drug-target-indication relationship for
650 available repurposed drugs. *Computational and Structural Biotechnology Journal* 18, 1043 – 1055
- 651 Partl, C., Gratzl, S., Streit, M., Wassermann, A. M., Pfister, H., Schmalstieg, D., et al. (2016). Pathfinder:
652 Visual analysis of paths in graphs. *Computer Graphics Forum* 35, 71–80
- 653 Pillai, M. and Wu, D. (2024). Validation approaches for computational drug repurposing: a review. In
654 *AMIA Annual Symposium Proceedings*. vol. 2023, 559
- 655 Pinzi, L., Bisi, N., and Rastelli, G. (2024). How drug repurposing can advance drug discovery: challenges
656 and opportunities. *Frontiers in Drug Discovery* 4, 1460100
- 657 Preiss, J. (2025). A hybrid approach to literature-based discovery: combining traditional methods with
658 llms. *Applied Sciences* 15, 8785
- 659 Pushpakom, S., Iorio, F., Eyers, P. A., Escott, K. J., Hopper, S., Wells, A., et al. (2019). Drug repurposing:
660 progress, challenges and recommendations. *Nature reviews Drug discovery* 18, 41–58

- 661 Santamaría, L. P., Carro, E. U., Uzquiano, M. D., Ruiz, E. M., Gallardo, Y. P., and Rodríguez-González, A.
662 (2021). A data-driven methodology towards evaluating the potential of drug repurposing hypotheses.
663 *Computational and Structural Biotechnology Journal* 19, 4559–4573
- 664 Saranraj, K. and Kiran, P. U. (2025). Drug repurposing: Clinical practices and regulatory pathways.
665 *Perspectives in Clinical Research* 16, 61–68
- 666 Schatz, K., Melo-Filho, C., Tropsha, A., and Chirkova, R. (2021). Explaining drug-discovery hypotheses
667 using knowledge-graph patterns. In *2021 IEEE International Conference on Big Data (Big Data)*.
668 3709–3716. doi:10.1109/BigData52589.2021.9672006
- 669 Seagle, H. M., Akerele, A. T., DeCorte, J. A., Hellwege, J. N., Breeyear, J. H., Kim, J., et al.
670 (2025). Genomics-informed drug repurposing strategy identifies novel therapeutic targets for metabolic
671 dysfunction-associated steatotic liver disease. *medRxiv*
- 672 Shefchek, K. A., Harris, N. L., Gargano, M., Matentzoglou, N., Unni, D., Brush, M., et al. (2019). The
673 monarch initiative in 2019: an integrative data and analytic platform connecting phenotypes to genotypes
674 across species. *Nucleic Acids Research* 48, D704–D715. doi:10.1093/nar/gkz997
- 675 Sikirzhyskaya, A., Tyagin, I., Sutton, S. S., Wyatt, M. D., Safro, I., and Shtutman, M. (2025). Ai-
676 based mining of biomedical literature: Applications for drug repurposing for the treatment of dementia.
677 *Artificial Intelligence in Medicine* , 103218
- 678 Steyaert, S., Pizurica, M., Nagaraj, D., Khandelwal, P., Hernandez-Boussard, T., Gentles, A. J., et al.
679 (2023). Multimodal data fusion for cancer biomarker discovery with deep learning. *Nature machine*
680 *intelligence* 5, 351–362
- 681 Sun, S., Shyr, Z., McDaniel, K., Fang, Y., Tao, D., Chen, C. Z., et al. (2025). Reversal gene expression
682 assessment for drug repurposing, a case study of glioblastoma. *Journal of Translational Medicine* 23,
683 25
- 684 Tanoli, Z., Fernández-Torras, A., Özcan, U. O., Kushnir, A., Nader, K. M., Gadiya, Y., et al. (2025).
685 Computational drug repurposing: approaches, evaluation of in silico resources and case studies. *Nature*
686 *Reviews Drug Discovery* 24, 521–542. doi:10.1038/s41573-025-01164-x
- 687 Thakur, G., Anish, Chaudhary, S., and Verma, K. K. (2024). Drug repurposing and its various approaches.
688 *International Journal For Multidisciplinary Research*
- 689 Thorman, A. W., Reigle, J., Chutipongtanate, S., Yang, J., Shamsaei, B., Pilarczyk, M., et al. (2024).
690 Accelerating drug discovery and repurposing by combining transcriptional signature connectivity with
691 docking. *Science Advances* 10, eadj3010
- 692 U.S. National Library of Medicine (2025). Medical subject headings (mesh). <https://meshb.nlm.nih.gov/>. National Institutes of Health. Accessed: 2025-10-08
- 694 Wang, Q., Huang, K., Chandak, P., Gehlenborg, N., and Zitnik, M. (2021). Interactive visual explanations
695 for deep drug repurposing. In *Workshop on Interpretable Machine Learning in Healthcare at*
696 *International Conference on Machine Learning (ICML)*. 5 pages
- 697 Wang, Q., Huang, K., Chandak, P., Zitnik, M., and Gehlenborg, N. (2022). Extending the nested model for
698 user-centric xai: A design study on gnn-based drug repurposing. *IEEE Transactions on Visualization*
699 *and Computer Graphics* 29, 1266–1276
- 700 Wishart, D. S., Knox, C., Guo, A. C., Cheng, D., Shrivastava, S., Tzur, D., et al. (2008). Drugbank: a
701 knowledgebase for drugs, drug actions and drug targets. *Nucleic acids research* 36, D901–D906
- 702 Xu, P., Ding, Y., and Fan, W. (2024). Chartadapter: Large vision-language model for chart summarization.
703 *arXiv preprint arXiv:2412.20715*

- 704 Yu, K., Jiang, R., Zhou, D., and Zhao, Z. (2024). Therapeutic targets for alzheimer's disease:
705 Proteome-wide mendelian randomization and colocalization analyses. *Journal of Alzheimer's Disease* ,
706 13872877251344572
- 707 Zang, C., Zhang, H., Xu, J., Zhang, H., Fouladvand, S., Havaladar, S., et al. (2023). High-throughput target
708 trial emulation for alzheimer's disease drug repurposing with real-world data. *Nature communications*
709 14, 8180
- 710 Zhang, Z., Chen, L., Zhong, F., Wang, D., Jiang, J., Zhang, S., et al. (2022). Graph neural network
711 approaches for drug-target interactions. *Current Opinion in Structural Biology* 73, 102327